remote sensing

MDPI

Article

Spatiotemporal Dynamics of Terrestrial Vegetation and Its Driver Analysis over Southwest China from 1982 to 2015

Chunhui Duan [1], Jinghao Li [1], Yanan Chen [1], Zhi Ding [1], Mingguo Ma [1], Jing Xie [2], Li Yao [1] and Xuguang Tang [1,*]

[1] Chongqing Jinfo Mountain Karst Ecosystem National Observation and Research Station, School of Geographical Sciences, Southwest University, Chongqing 400715, China; yhl5893663@163.com (C.D.); a852220431@163.com (J.L.); chenyanan_1998@163.com (Y.C.); dingzhi11@mails.ucas.ac.cn (Z.D.); mmg@swu.edu.cn (M.M.); yao66625@swu.edu.cn (L.Y.)

[2] School of Geography and Planning, Sun Yat-sen University, Guangzhou 510275, China; xiej95@mail.sysu.edu.cn

* Correspondence: xgtang@swu.edu.cn; Tel.: +86-23-6825-2370

Abstract: Global environmental changes have been dramatic recently, exerting substantial effects on the structures and functions of terrestrial ecosystems, especially for the ecologically-fragile karst regions. Southwest China is one of the largest karst continuum belts around the world, which also contributes about 1/3 of terrestrial carbon sequestration to China. Therefore, a deep understanding of the long-term changes of vegetation across Southwest China over the past decades is critical. Relying on the long time series of Advanced Very High Resolution Radiometer (AVHRR) Global Inventory Modeling and Mapping Studies normalized difference vegetation index (GIMMS NDVI3g) data set, this study examined the spatial and temporal patterns of vegetation conditions in Southwest China from 1982 to 2015, as well as their response to the environmental factors including temperature, precipitation and downward shortwave radiation. Multi-year mean NDVI showed that except the northwestern region, the NDVI of Southwest China was large, ranging from 0.5 to 0.8. Meanwhile, nearly 43.7% of the area experienced significant improvements in NDVI, whereas only 3.47% of the area exhibited significant decreases in NDVI. Interestingly, the NDVI in karst area increased more quickly with 1.035×10^{-3}/a in comparison with that in the non-karst area with about 0.929×10^{-3}/a. Further analysis revealed that temperature is the dominant environmental factor controlling the interannual changes in NDVI, accounting for 48.19% of the area, followed by radiation (3.71%) and precipitation (3.09%), respectively.

Keywords: vegetation dynamics; karst ecosystem; trend analysis; environmental driving factors

Citation: Duan, C.; Li, J.; Chen, Y.; Ding, Z.; Ma, M.; Xie, J.; Yao, L.; Tang, X. Spatiotemporal Dynamics of Terrestrial Vegetation and Its Driver Analysis over Southwest China from 1982 to 2015. *Remote Sens.* **2022**, *14*, 2497. https://doi.org/10.3390/rs14102497

Academic Editor: Ramón Alberto Díaz-Varela

Received: 25 April 2022
Accepted: 20 May 2022
Published: 23 May 2022

1. Introduction

Terrestrial vegetation directly connects the material cycle and energy flow among soil sphere, hydrosphere and atmosphere, playing an important role in regulating terrestrial carbon balance and climate system [1]. In recent decades, global environmental changes including climate change and human-induced disturbances have exerted substantial effects on vegetation structures and functions, particularly for ecologically-fragile terrestrial ecosystems [2–4]. Therefore, a deep understanding of the spatiotemporal dynamics of vegetation over large areas has important scientific value and practical significance for ecosystem management.

Vegetation monitoring is a long-term dynamic process, which is crucial to the current research on global and regional climate change and eco-environmental quality assessment [5,6]. Owing to the advantages of high temporal and spatial resolution, wide extent of coverage, good timeliness and large amount of information, satellite remote sensing technology has become the first choice for the dynamic detection of vegetation condition over a long period and broad extent [7,8]. Among vegetation information obtained from

remote sensing, the normalized difference vegetation index (NDVI) is of relatively wide usage [9], and can well reflect the variation of vegetation coverage, biomass and ecosystem parameters [10,11]. Due to these, it is widely used for monitoring vegetation dynamics from global to regional scale and its response to climate change.

At present, there are many remote sensing data sets that can provide NDVI products, such as Moderate Resolution Imaging Spectroradiometer (MODIS) NDVI, SPOT VGT, Advanced Very High Resolution Radiometer (AVHRR) Global Inventory Modeling and Mapping Studies (GIMMS) NDVI. In terms of the AVHRR GIMMS NDVI data set, it has the characteristics of long time series, wide coverage, comparable time and space, and strong representation ability of vegetation dynamics, which have been proved to be the optimal data sets to characterize long-term vegetation growth conditions [9,12]. Currently, the data have two generations including GIMMS NDVIg and GIMMS NDVI3g, which cover the periods of 1981–2006 and 1981–2015, respectively. Several studies have compared their differences from the perspectives of monitoring vegetation activity change in the Northern Hemisphere and extracting the information of vegetation phenology [13,14]. Generally, the NDVIg data set largely underestimated the changing trend of terrestrial vegetation by comparison with the new-released NDVI3g product [14–16].

The response of NDVI to environmental factors was crucial to understand the impact of global and regional changes on terrestrial ecosystems [17,18], and develop appropriate strategies to confront and settle the potential challenges [19], which was also one of the research hotspots in recent years. The growth of vegetation will consume substantial water during photosynthesis, and the availability of resources such as solar radiation and temperature will affect its use efficiency. Meanwhile, human activities can exert positive or negative effects on the structure and function of terrestrial ecosystems. Thus, the dynamics of vegetation are closely related to the environment changes from both climate variability and human-induced disturbance [20].

Southwest China has the largest karst area in China and is also one of the three largest karst concentrated contiguous areas in the world [21,22]. However, the karst ecosystems are facing serious ecological and socio-economic problem due to rocky desertification. In order to alleviate the problem, the government has implemented a series of ecological projects, promoting the vegetation productivity in karst areas [23]. Detecting vegetation change in the karst area can effectively reflect the condition and change of regional rocky desertification, which has important guiding significance. However, there is still a lack of long-term monitoring of vegetation dynamics in this ecologically-fragile region. In the study, using the long-time series AVHRR GIMMS NDVI3g data set, we aimed: (1) to figure out the spatial pattern of multi-year mean NDVI in Southwest China during the past four decades; (2) to examine the long-term changes in interannual NDVI across this region; and (3) to clarify the dominant environmental factor determining the dynamics in NDVI through the spatial partial correlation analysis.

2. Materials and Methods

2.1. Study Area

The study area is located in the Southwest China spanning from 20°54′N to 34°19′N and from 91°21′E to 112°04′E, covering an area of about 1.36 million km^2, which is composed of the five provinces Sichuan, Chongqing, Guizhou, Yunnan and Guangxi (Figure 1). In general, this region is characterized by complex topography and diverse landform. Meanwhile, this area is the most concentrated and typical karst landform distribution area in China with an area of 0.55 million km^2, which is also one of the three largest karst regions in the world [24]. The climate type of most areas in Southwest China is subtropical monsoon climate. Annual mean precipitation is generally above 900 mm but unevenly distributed in months, with 80–90% falling from May to October [25]. Additionally, more than 48% of the surface in Southwest China is covered by forest, about 18% is grassland and about 2% is shrubland.

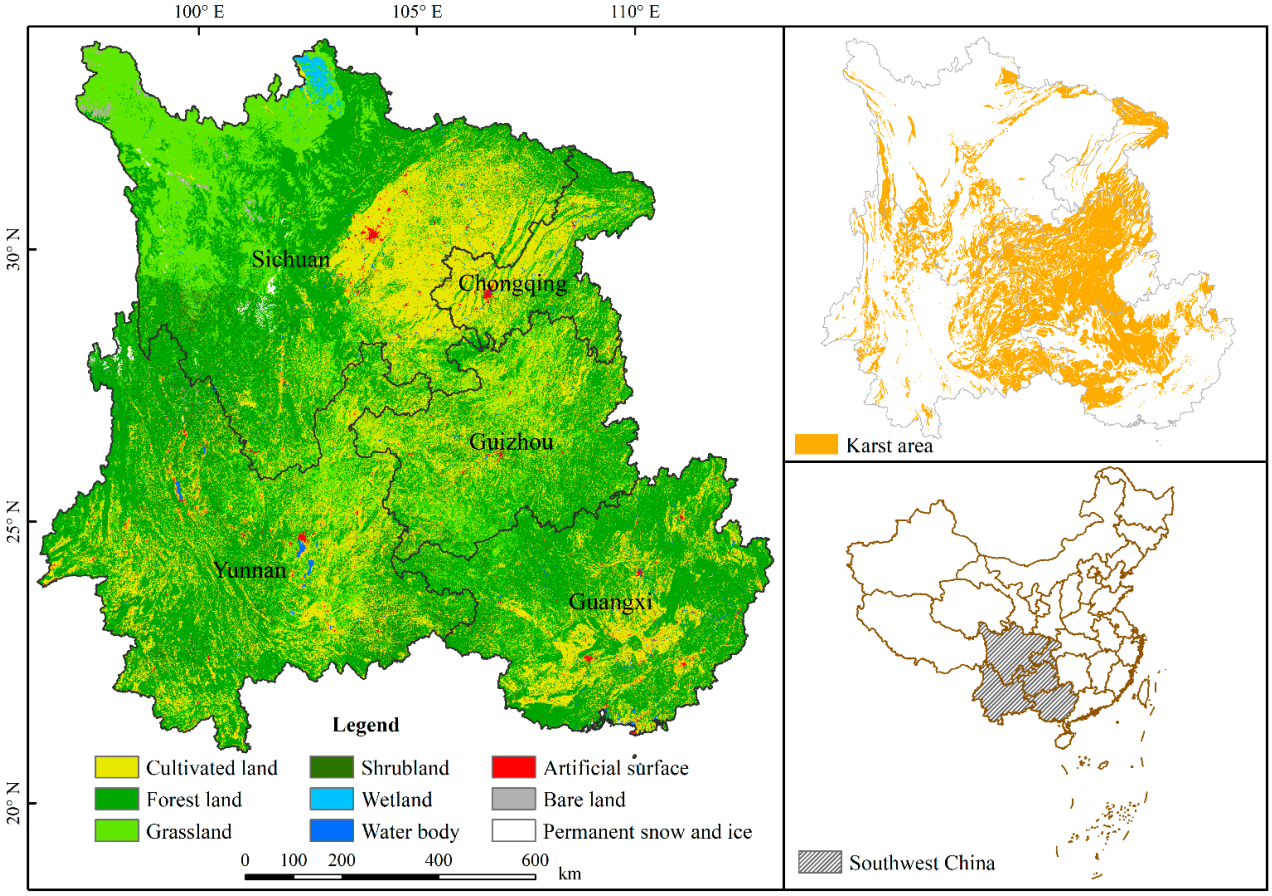

Figure 1. The map of land use/land cover in Southwest China and distribution of karst ecosystem.

2.2. Data Sets

2.2.1. AVHRR GIMMS NDVI3g Data

For a long time, the most commonly used NDVI data has been the GIMMS NDVIg dataset from 1981 to 2006 [16]. To study the vegetation dynamics beyond 2006, it needs to be expanded with other data sets such as MODIS NDVI data. A new updated version of the AVHRR GIMMS NDVI3g data set is now available [26] covering from 1981 to 2015, which specifically aims to improve the data quality in the high latitudes of Northern Hemisphere [15]. This long record is comprised of data from two different sensors: AVHRR/2 (from July 1981 to November 2000) and AVHRR/3 (from November 2000 to the present) [26]. The empirical mode decomposition/reconstruction was employed to minimize varying solar zenith angle effects introduced by orbital drift, when producing GIMMS NDVI3g [27]. In this study, we used the GIMMS NDVI3g data for analysis with the spatial resolution of 1/12 degree and temporal resolution of 15 days, and the maximum value composite method was applied to process into monthly data. It can be obtained from the NASA Ames Ecological Forecasting Lab (https://ecocast.arc.nasa.gov/data/pub/gimms/3g.v1/) (accessed on 23 April 2021).

Due to the relatively coarse resolution of GIMMS NDVI3g, the MODIS NDVI (MOD13A3) data with a spatial resolution of 1 km and a temporal resolution of 1 month from 2001 to 2015 was employed to evaluate the consistence to GIMMS NDVI3g over Southwest China. As shown in Figure 2, the coefficient of determination (R^2) between GIMMS NDVI3g and MODIS NDVI reached up to 0.99. Many previous studies have also conducted the comparison between GIMMS NDVI3g and MODIS NDVI, and found that the trends of GIMMS NDVI3g were basically consistent with MODIS NDVI data [28–30]. The MODIS NDVI can be obtained from the LAADS DAAC (https://ladsweb.modaps.eosdis.nasa.gov/) (accessed on 14 May 2022).

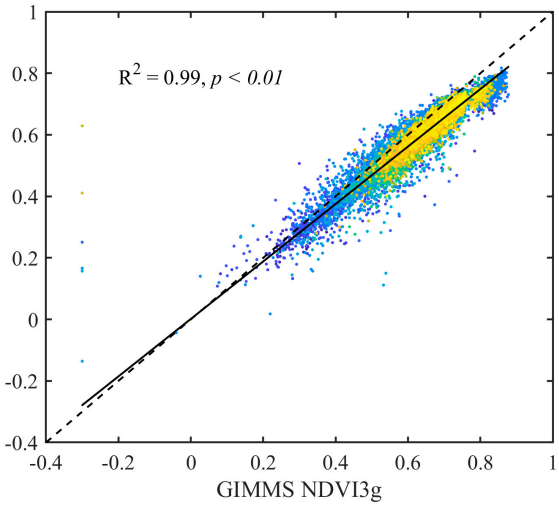

Figure 2. The scatter diagram of multi-year mean NDVI between GIMMS NDVI3g and MODIS NDVI in pixel level.

2.2.2. Meteorological Data

The meteorological data, including temperature, precipitation and downward shortwave radiation data, are derived from the China Meteorological Forcing Dataset (CMFD) with a spatial resolution of 0.1 degree, a temporal resolution of 3 h; its record begins in January 1979, currently extending up to December 2018, and can be obtained from Big Earth Data for Three Poles (https://poles.tpdc.ac.cn/zh-hans/) (accessed on 23 April 2021). The CMFD data was made through fusion of remote sensing products, reanalysis datasets and in-situ station data, and formed the first high spatial-temporal resolution gridded near-surface meteorological dataset for studies of land surface processes in China [31]. The reanalysis and remote sensing data used were Global Land Data Assimilation System (GLDAS) NOAH10SUBP 3H, GLDAS NOAH025 3H, Modern Era Retrospective-Analysis for Research and Applications (MERRA) MAI3CPASM 5.2.020, Global Energy and Water Exchanges-Surface Radiation Budget (GEWEX-SRB) REL3.0 SW 3HRLY21 and Tropical Rainfall Measuring Mission (TRMM) 3B42 v7. The ground-based observations were from two sources including the China Meteorological Administration (CMA) data and the National Oceanic and Atmospheric Administration (NOAA)'s National Centers for Environmental Information (NCEI) data. The values of non-physical range, which emerge when the interpolation algorithm is employed to create gridded data from the station observation data, were removed before using ANU-Spline statistical interpolation, such as negative value of gridded precipitation and downward shortwave radiation data interpolated from the CMA/NCEI data. The accuracy lies between the observation data and satellite remote sensing data, which is superior to the existing international reanalysis data [32], indicating that fusing both the surface observation estimates and the satellite estimates will apparently improve the estimation accuracy [31].

2.2.3. Land Cover Data

In the study, we used the time-series land cover data set (1982–2018) from Global Land Surface Satellite (GLASS) to investigate its effect on the spatio-temporal change of NDVI. Using China land use/cover data sets (CNLUCC). This data set established the corresponding relationship between land cover samples and GLASS quantitative remote sensing products. The bidirectional long-term and short-term memory network (Bi-LSTM) model in the TensorFlow framework based on Python was employed for model training and prediction [33]. The overall accuracy of the data set was up to 84.2%. The spatial resolution is 0.05°, which can be obtained from National Earth System Science Data Center, China (http://www.geodata.cn) (accessed on 14 May 2022). In the study, land cover was

divided into the following 9 types: cultivated land, forest land, grassland, shrubland, wetland, water body, artificial surface, bare land and permanent snow and ice.

2.3. Analysis

2.3.1. Data Preprocess

As a result of the rainy and cloudy climate in Southwest China, there exists a series of noises in the NDVI data. In order to eliminate potential residual effects of cloud, smog or other noise [4], the maximum value composite is one of the most commonly used algorithms [34]. In the study, we adopted this algorithm to process the raw AVHRR GIMMS NDVI3g data at a 15-day interval, aggregating the monthly data. The formula is as follows:

$$MNDVI_i = Max(NDVI_1,\ NDVI_2) \tag{1}$$

where $MNDVI_i$ is monthly value of NDVI; i is month, i = 1, 2, . . . , 12; $NDVI_1$ is the first half of each month, and $NDVI_2$ is the second half of each month. The technique selected the larger NDVI value from the two images pixel by pixel, taking it as the value of the corresponding pixel in the monthly image. The output image minimized cloud contamination, sun-angle and shadow effects and aerosol and water-vapor effects; meanwhile, the directional reflectance and off-nadir viewing effects were also reduced [35].

2.3.2. Trend Analysis

The trend analysis method refers to the analysis of the change trend of the relevant indicators in long-term sequence. In the study, trend analysis was applied to investigate the NDVI change tendency from regional and pixel scale. The formula is as follows:

$$\theta_{slope} = \frac{n \times \sum_{i=1}^{n} i \times M_{NDVI_i} - \sum_{i=1}^{n} i \sum_{i=1}^{n} M_{NDVI_i}}{n \sum_{i=1}^{n} i^2 - \left(\sum_{i=1}^{n} i\right)^2} \tag{2}$$

where θ_{slope} is the slope of the NDVI trend; n is the number of cumulative years of monitoring period; i = 1 represents the year 1982; $MNDVI_i$ is the maximum NDVI of the pixel in year i. The larger $|\theta_{slope}|$ is, the more obvious the variation of NDVI is. When $\theta_{slope} < 0$, it indicates that vegetation exhibits a decreasing trend; otherwise, when $\theta_{slope} > 0$, it shows an increasing trend. The significance test is essential for long-time trend analysis. In this study, the significance of the NDVI trend was examined by F test at a confidence level of 95%.

2.3.3. Partial Correlation Analysis

Partial correlation analysis aims to eliminate the influence of the third variable, and only analyze the correlation between the two variables. In the study, partial correlation analysis was performed to investigate the response of NDVI to temperature, precipitation and downward shortwave radiation. The formula is as follows:

$$R_{12(3)} = \frac{R_{12} - R_{13}R_{23}}{\sqrt{1 - R_{13}^2}\sqrt{1 - R_{23}^2}} \tag{3}$$

where $R_{12(3)}$ is the partial correlation coefficient between factor 1 and factor 2 with factor 3 controlled, and R_{12}, R_{13} and R_{23} are the correlation coefficients between factor 1, 2 and 3, respectively. In the study, the significance level (p-value) was the criterion to determine the dominant environmental factors. While one of them passed the significance test ($p < 0.05$) but other two did not, the former was the dominant factors; while two of them passed but the third did not, both were the dominant factors; while all of them passed, all of them were the dominant factors; while none of them passed, these pixels were viewed as having no dominant environmental factors. In the study, we performed the data analysis with Python and ArcGIS.

3. Results

3.1. Spatial Pattern

In general, multi-year mean NDVI over Southwest China from 1982 to 2015 showed a decreasing trend from the southeastern to the northwestern (Figure 3). High vegetation-covered areas (0.7~0.9) with an area ratio about 18.49% were mainly distributed in southwestern Yunnan, northern Guangxi and central Sichuan. Low vegetation-covered areas (0.2~0.4) with an area ratio about 3.64% mainly appeared in western Sichuan, which is related to huge relief degree of land surface and relatively high altitude with harsh climate. Multi-year mean NDVI over Southwest China ranged majorly from 0.5 to 0.8, accounting for about 83.90%, and the mean NDVI was 0.61 for the whole region, which indicated that the overall vegetation condition in Southwest China was relatively well. In addition, the area of multi-year mean NDVI being lower than 0.2 only accounted for 0.18%.

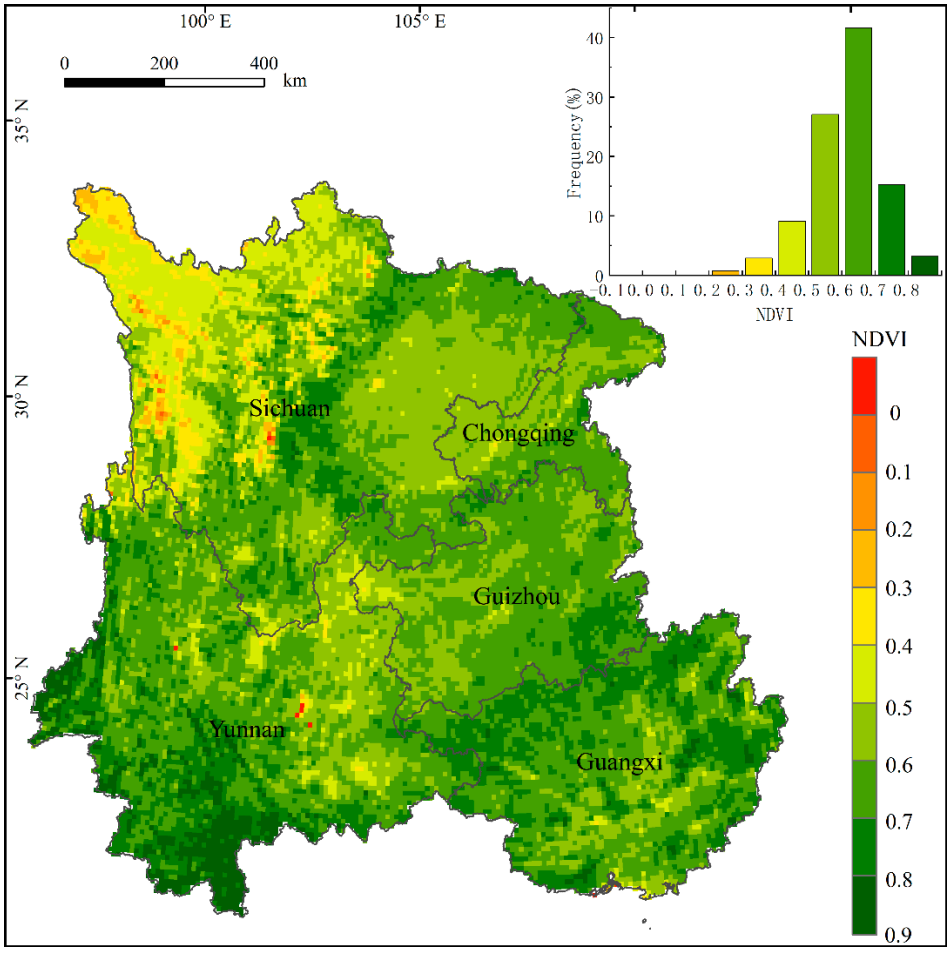

Figure 3. Spatial pattern of multi-year mean NDVI over Southwest China from 1982 to 2015.

As shown in Figure 4 and Table 1, generally, the vegetation types in Southwest China were comprised of forest land, grassland, cultivated land and shrubland. Overall, forest land was the main contributor of vegetation NDVI, and exhibited an apparent increase in area from 1982 to 2015 by 14.19%. Meanwhile, the areas of grassland, cultivated land and shrubland decreased about 6.09%, 7.84% and 11.07%, respectively. However, the magnitudes of both increase and reduction were basically equal. Nevertheless, the regional mean NDVI value in 2015 increased significantly by 7.28% in comparison with that in 1982. Table 2 also indicated that the area of NDVI ranging from 0.6 to 0.9 has increased from 68.26×10^4 km to 98.07×10^4 km, while the area of NDVI ranging from 0.2 to 0.6 has decreased from 67.46×10^4 km to 37.64×10^4 km since 1982 to 2015. It proved that the quality of vegetation improved obviously during the past decades.

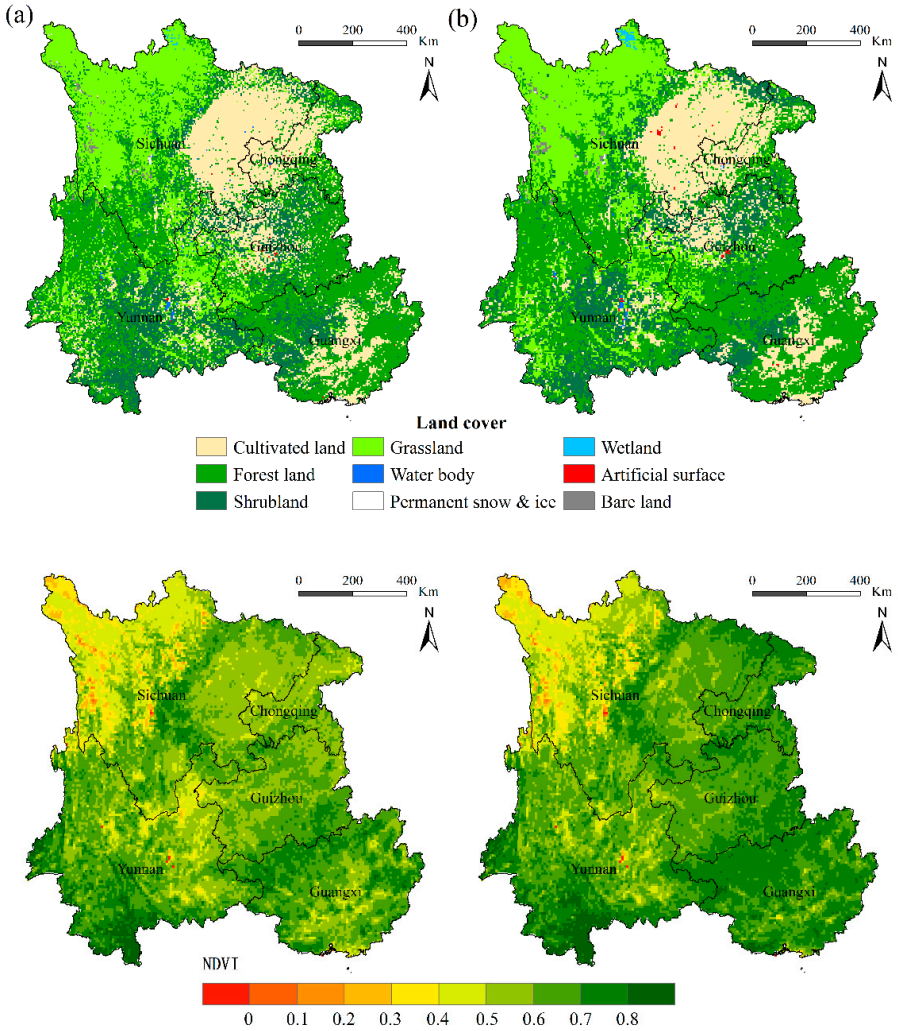

Figure 4. Comparison of the land cover and spatial pattern of NDVI in 1982 (**a**) and 2015 (**b**).

Table 1. Changes of land cover between 1982 and 2015.

Land Cover	1982 ($\times 10^4$ km)	2015 ($\times 10^4$ km)	Rate of Change (%)
Cultivated land	29.68	27.35	−7.84
Forest land	48.47	55.37	14.19
Shrubland	24.19	21.52	−11.07
Grassland	32.37	30.40	−6.09
Water body	0.35	0.22	−38.46
Permanent snow and ice	0.10	0.05	−42.86
Wetland	0.08	0.26	216.67
Artificial surface	0.14	0.18	30.00
Bare land	0.63	0.67	6.52

Table 2. Changes of NDVI in different range between 1982 and 2015.

NDVI	1982 ($\times 10^4$ km)	2015 ($\times 10^4$ km)	Rate of Change (%)
<0	0.05	0.07	25.00
0–0.1	0.07	0.04	−40.00
0.1–0.2	0.16	0.18	8.33
0.2–0.3	1.37	1.16	−15.84
0.3–0.4	4.84	3.97	−17.98
0.4–0.5	16.96	11.49	−32.24
0.5–0.6	44.28	21.03	−52.49
0.6–0.7	48.40	55.24	14.17
0.7–0.8	16.70	38.52	130.62
>0.8	3.16	4.31	36.64

3.2. Long-Term Trend

Generally, NDVI in Southwest China from 1982 to 2015 showed a significant increasing trend with a rate of 0.936 × 10^{-3}/a (Figure 5). Meanwhile, it presented a decreasing trend from the eastern to the western. The maximum trend value appeared in central Sichuan, while the minimum trend value appeared in central Guangxi. Approximately 77.96% of the area exhibited a positive trend, especially in northeastern Sichuan, Chongqing and Guangxi, while approximately 22.04% of the area exhibited a negative trend, mainly in western Sichuan, and northwestern and central Yunnan (Figure 5). Besides, the NDVI values of cultivated land, forest land, grassland and shrubland have increased significantly at 1.107 × 10^{-3}/a, 0.89 × 10^{-3}/a, 0.509 × 10^{-3}/a and 0.827 × 10^{-3}/a, respectively (Figure 6), which jointly explain the increase in vegetation NDVI over Southwest China from 1982 to 2015.

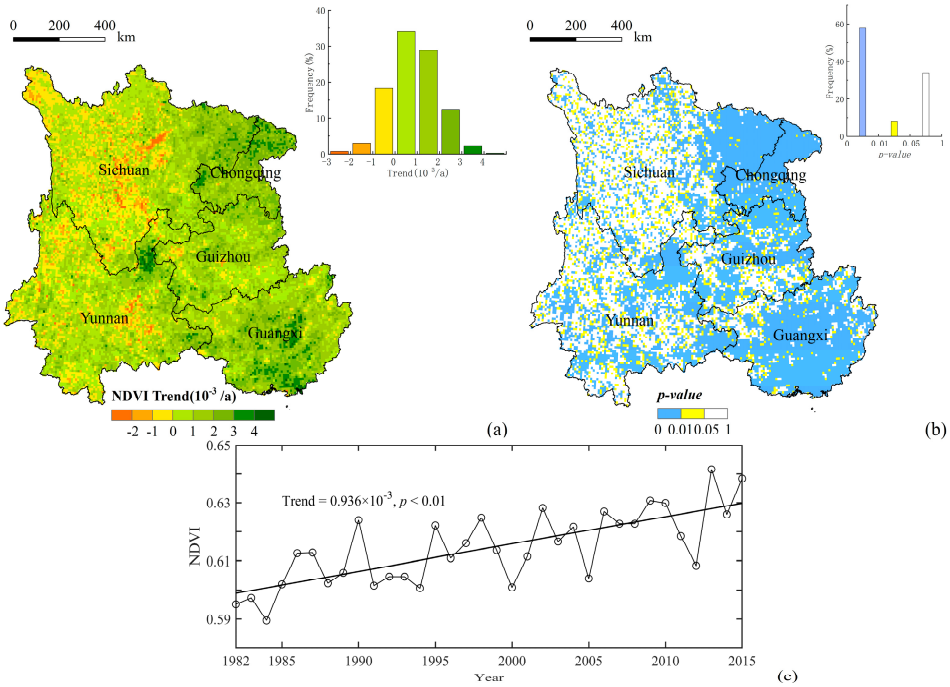

Figure 5. Spatial trend analysis of vegetation NDVI (**a**), the associated significant level (**b**) and linear regressions of NDVI (**c**) over Southwest China from 1982 to 2015.

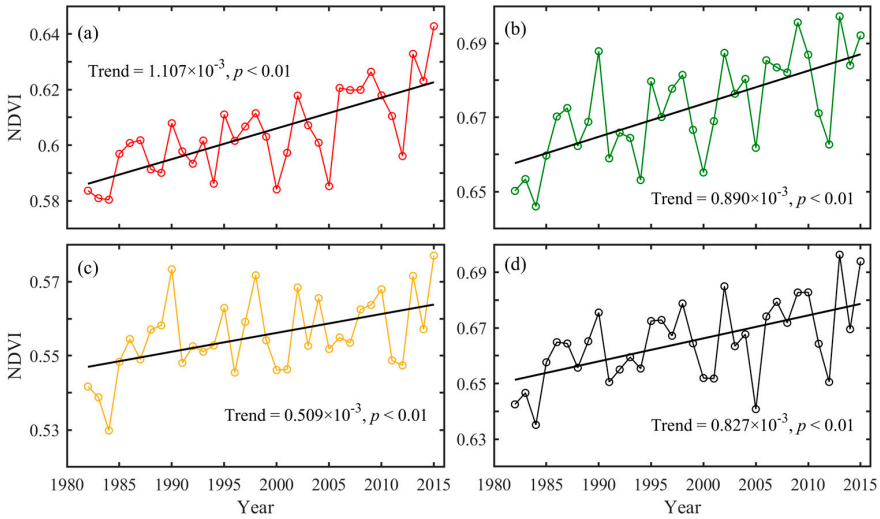

Figure 6. The long-term trend of NDVI of cultivated land (**a**), forest land (**b**), grassland (**c**) and shrubland (**d**) over Southwest China from 1982 to 2015.

The areas of significant increase and slight increase over Southwest China during 1982–2015 were 50.14% and 8.61%, respectively (Table 3), with the concentrated distribution area mainly lying in the eastern region (Figure 7), whereas the area of significant reduction and slight reduction were 3.29% and 2.49% respectively, distributing sparsely in the northwestern and central areas. In addition, 35.48% of the whole region seems stable.

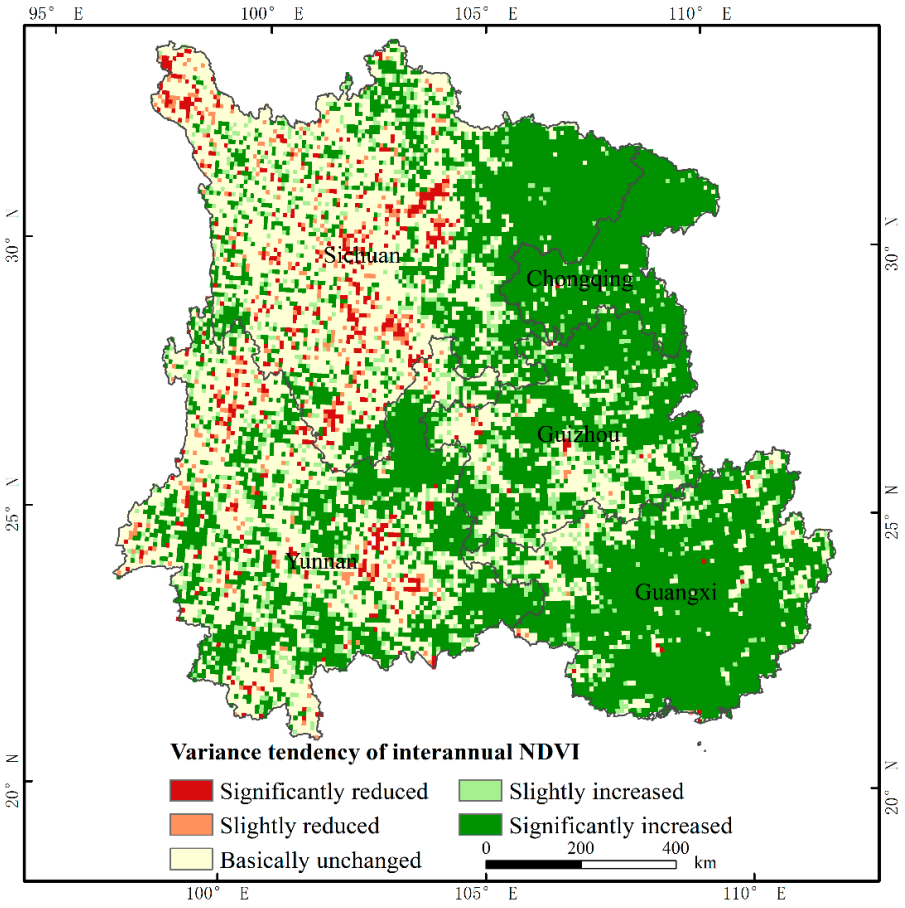

Figure 7. Variance tendency of interannual NDVI over Southwest China from 1982 to 2015.

Table 3. The area ratio of different variance tendency of NDVI over Southwest China during 1982–2015.

Variance Tendency	*p*-Value	Ratio (%)
Significantly reduced	$p < 0.01$	3.29
Slightly reduced	$0.01 \leq p < 0.05$	2.49
Basically unchanged	$p \geq 0.05$	35.48
Slightly increased	$0.01 \leq p < 0.05$	8.61
Significantly increased	$p < 0.01$	50.14

3.3. Driving Factor Analysis

In the study, spatial partial correlation analysis was used in order to dig out the response of vegetation NDVI to climatic factors including air temperature, precipitation and downward shortwave radiation (Figures 8 and 9). Overall, the area controlled by temperature was about 48.19% ($p < 0.05$), followed by downward shortwave radiation (3.71%, $p < 0.05$) and precipitation (3.09%, $p < 0.05$). Meanwhile, the area controlled by both temperature and precipitation was about 4.60% ($p < 0.05$), followed by both temperature and downward shortwave radiation (3.80%, $p < 0.05$). Approximately 35.47% of the area showed none of climatic controlling factors owing to insignificant changes in NDVI over the past four decades (Figure 9). Moreover, the pixels with significant positive partial correlation between temperature and NDVI were mainly concentrated in the eastern regions, while

few pixels in the western regions showed significant negative partial correlation. The pixels with significant positive partial correlation between precipitation and NDVI were mainly distributed in southwest Chongqing and northwest and northeast Yunnan. The pixels in the western regions presented a large area of negative partial correlation between solar radiation and NDVI, particularly in the central and north Yunnan (Figure 8).

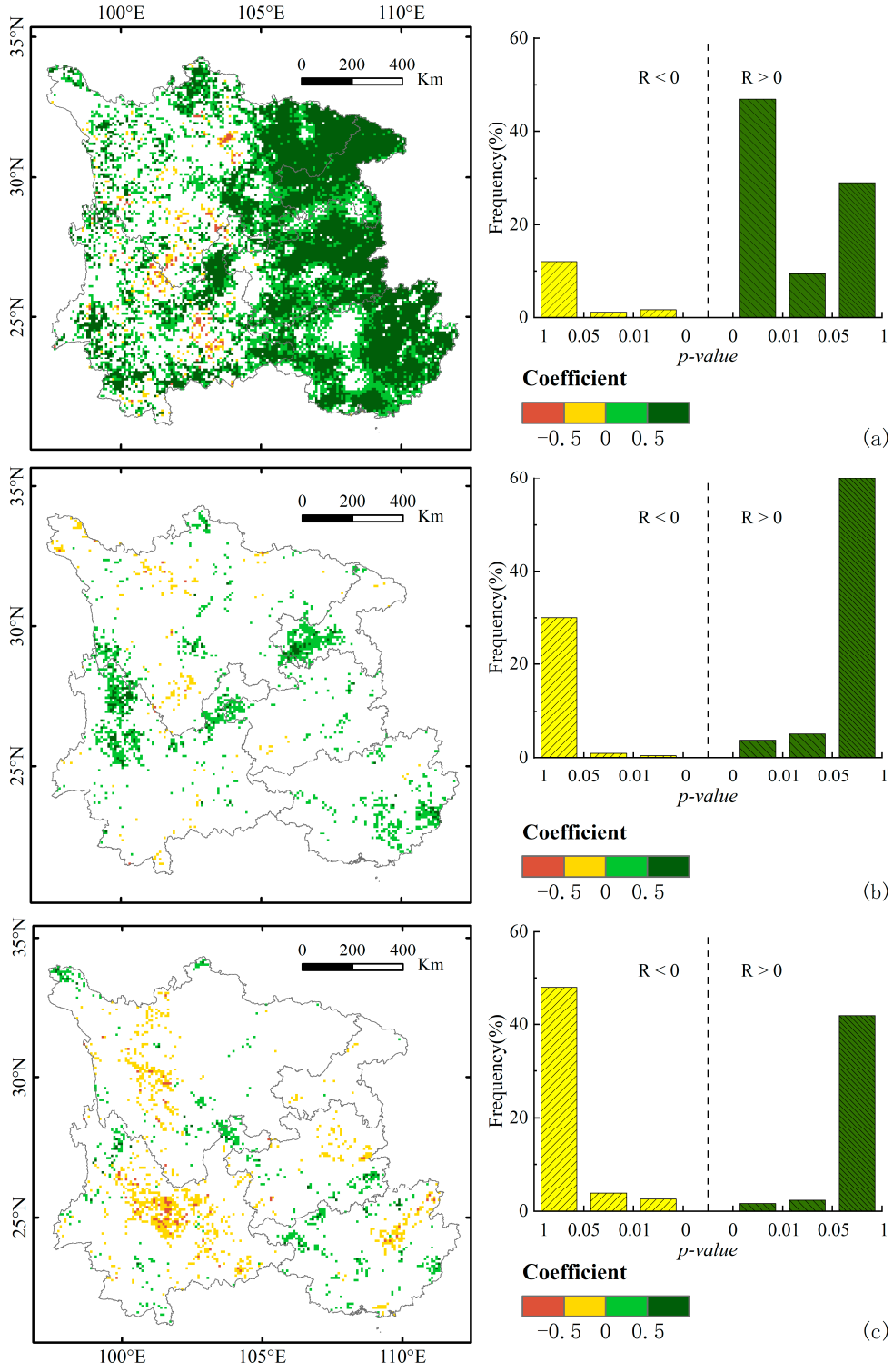

Figure 8. Spatial partial correlation analysis of NDVI and the associated environmental factors including temperature (**a**), precipitation (**b**) and downward shortwave radiation (**c**) across Southwest China during 1982–2015.

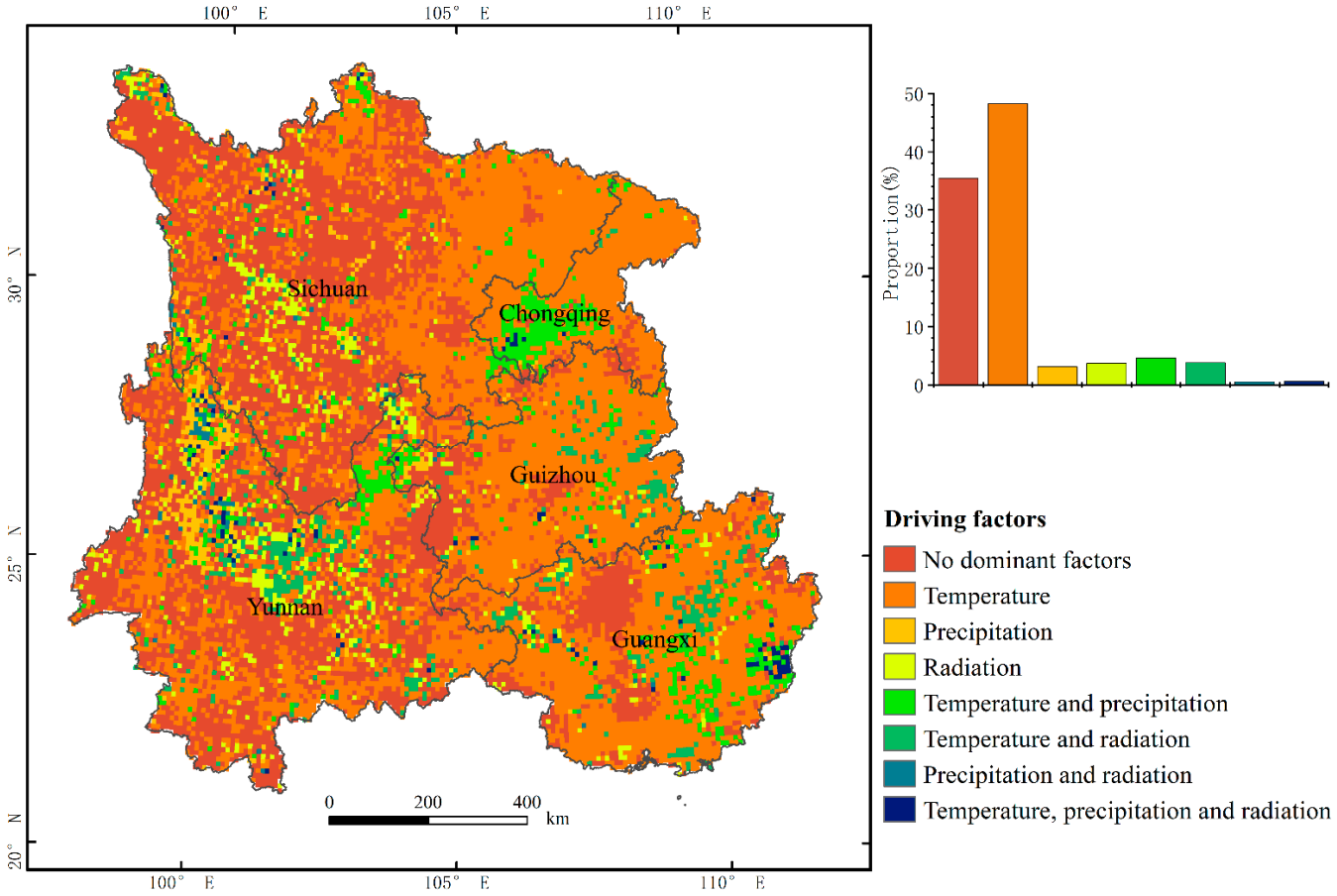

Figure 9. Spatial distribution of the dominant environmental factors over Southwest China during 1982–2015.

4. Discussion

4.1. Effects of Climate Factors

Many studies have investigated the response of vegetation NDVI to climatic factors on global [36], country [37] and regional [38,39] scales. Generally, as precipitation increases, vegetation flourishes. However, the areas controlled by precipitation was scarce in Southwest China. More than a half of the area was controlled by temperature during 1982–2015, which was consistent with previous findings [40,41]. Overall, precipitation is relatively abundant in Southwest China, which means precipitation is not a limiting factor. Under this circumstance, vegetation grow better owing to increased photosynthesis [42] and the growing season is lengthened [43] caused by increased temperature. In western Sichuan and central and north Yunnan, partial correlation coefficient between downward shortwave radiation and NDVI was negative, which was ascribed to low soil moisture brought about by increased evapotranspiration in a dry environment, with rising solar radiation [44].

In addition, some studies illustrated that the response of vegetation NDVI in the karst area is more sensitive to temperature than that in the non-karst area [45,46], which was the same with our study (Table 4). Some studies pointed out that the vegetation greening was driven principally by the elevation-dependent climate warming [47]. Karst landform is widely distributed in some high-latitude regions such as Yunnan-Guizhou plateau, therefore vegetation NDVI in the karst areas will be more susceptible to increasing temperature.

Table 4. Comparison of the area proportion in driving factors between the karst area and non-karst area over Southwest China from 1982 to 2015.

Environmental Factors	Karst Area	Non-Karst Area
No dominant factors	29.59	38.08
Temperature	55.99	44.70
Precipitation	2.79	3.23
Radiation	2.39	4.30
Temperature and Precipitation	4.42	4.70
Temperature and Radiation	4.02	3.70
Precipitation and Radiation	0.46	0.57
Temperature, Precipitation and Radiation	0.35	0.71

4.2. Differences in Vegetation NDVI between Karst and Non-Karst Areas

There existed many discrepancies in climatic, geological, geomorphological and socioeconomic circumstances between the karst and non-karst areas. It was the diversity within such conditions that led to the differences in vegetation NDVI [48,49]. Previous studies found that compared with the non-karst area, the improvement of vegetation performed better than that of the non-karst area in Southwest China [42,45,46].

In the study, the overall NDVI trends in the karst and non-karst areas over Southwest China from 1982 to 2015 exhibited significant increasing trends at rates of 1.035×10^{-3}/a and 0.929×10^{-3}/a, respectively (Figure 10), but the trend in the karst area is slightly stronger. Interestingly, the NDVI trend between the karst area and non-karst area in different ranges showed opposite characteristics (Figure 11a). When the trend value was higher than 1×10^{-3}/a, the proportion in each range of the karst area was larger than that of the non-karst area. On the contrary, when the trend value was lower than 1×10^{-3}/a, it exhibited the opposite condition. Meanwhile, the area ratios of significant increase and slight increase in the karst area were 59.33% and 9.20%, respectively, and the values were 46.05% and 8.37% in the non-karst area, respectively (Figure 11b). Nevertheless, some studies suggested a larger NDVI increasing trend does not mean the net primary productivity (NPP) value with similar dynamics [50]. This inspired us to pay more attention to the synthetic analysis on vegetation using NDVI and NPP.

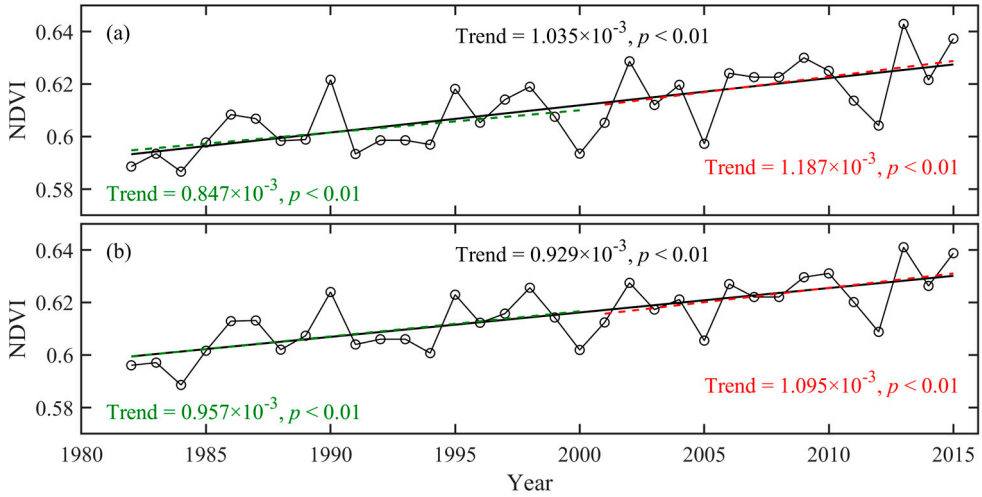

Figure 10. Long-term linear trend of vegetation NDVI in karst area (**a**) and non-karst area (**b**) over Southwest China from 1982 to 2015. The regressions from 1982 to 2015, 1982 to 2000 and 2001 to 2015 are labeled in black, green and red, respectively.

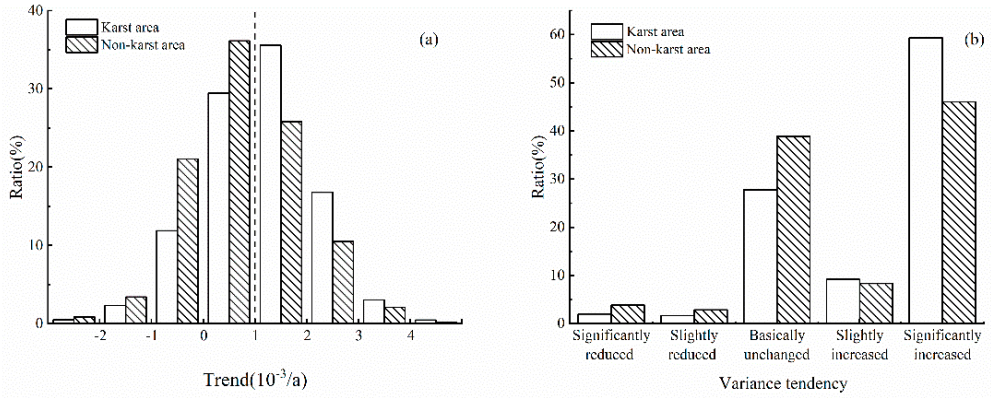

Figure 11. Comparisons of NDVI trend in different ranges (**a**) and variance tendency (**b**) between karst area and non-karst area in Southwest China from 1982 to 2015.

4.3. Impact of Human Activities

Human activities such as ecological projects can exert substantial effects on vegetation dynamics [22]. Since 2000, the national and local governments have implemented a series of ecological restoration projects, such as "the Grain for Green Program", "Natural Forest Protection Project" and "Karst Rocky Desertification Restoration Project" throughout Southwest China. The overall NDVI trends from 1982 to 2000 in the karst area and the non-karst area were 0.847×10^{-3}/a and 0.957×10^{-3}/a, respectively, neither of which passed the significance test (Figure 10). However, from 2001 to 2015, the trends were 1.187×10^{-3}/a and 1.095×10^{-3}/a, respectively, both of which were significant at a level of 0.05 (Figure 10). Significant changes between the two periods can be found in Figure 12. Furthermore, the transformation among land covers was of extreme importance for the vegetation dynamics. Widespread forest land, grassland and shrubland converted from cultivated land dominated the regional land cover changes [51,52]. Such change happened in China enlarged vegetation cover and restored vegetation productivity in the ecologically-fragile areas [23].

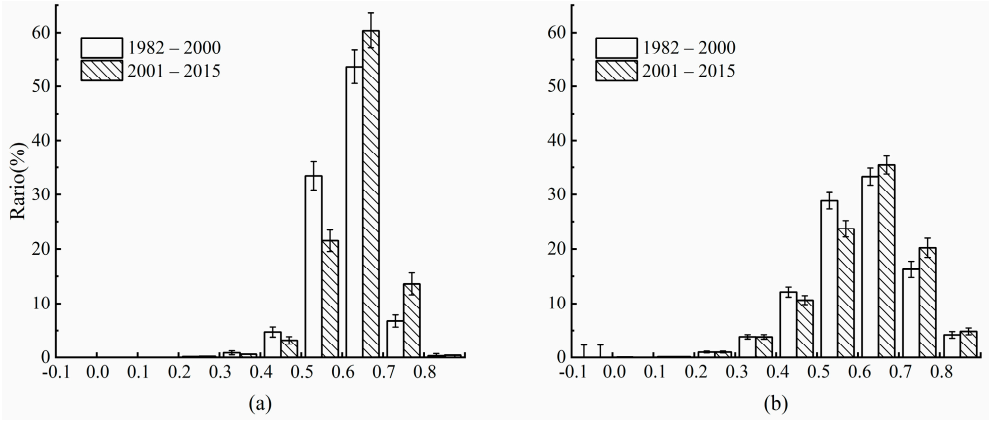

Figure 12. Comparisons of vegetation NDVI before and after the implementation of ecological projects during about 2000 in Southwest China: (**a**) Karst area and (**b**) non-karst area.

Figure 11 indicates that the NDVI trend and variance tendency differed a lot during the two periods. Since 2000, the eastern area has been experiencing significantly increasing tendency, while the western area has converted from significant increase to significant or slight reduction. This can be partly explained by the impact of annually sustained droughts [53]. Several studies have revealed a significant decreasing trend of precipitation in Southwest China after 2000 [47,54], and a drying trend was detected with moderate and severe droughts [55]. Moreover, the occurrence frequency and severity of droughts were rising in recent years [24]. Nevertheless, vegetation mainly presented a significant growing trend, especially for the eastern area (Figure 13). It proved that drought events

had not changed the greening trend of vegetation in Southwest China [56], which can be partly attributed to the implementation of a series of ecological restoration projects after 2000 [41,57]. Large-scale ecological restoration projects have also been recognized as the main reason for the vegetation greening in the karst area of Southwest China [39,42,58], whereas climate is the dominant driver of negative vegetation trends in non-karst areas [49]. However, large-scale afforestation may increase vegetation transpiration and consume more water resource, making vegetation coverage decrease [59]. Peng et al. [60] found that the positive effect of ecological engineering on vegetation productivity can be weakened by changing climate. Consequently, we should comprehensively investigate the natural and human-induced factors in dominating vegetation dynamics.

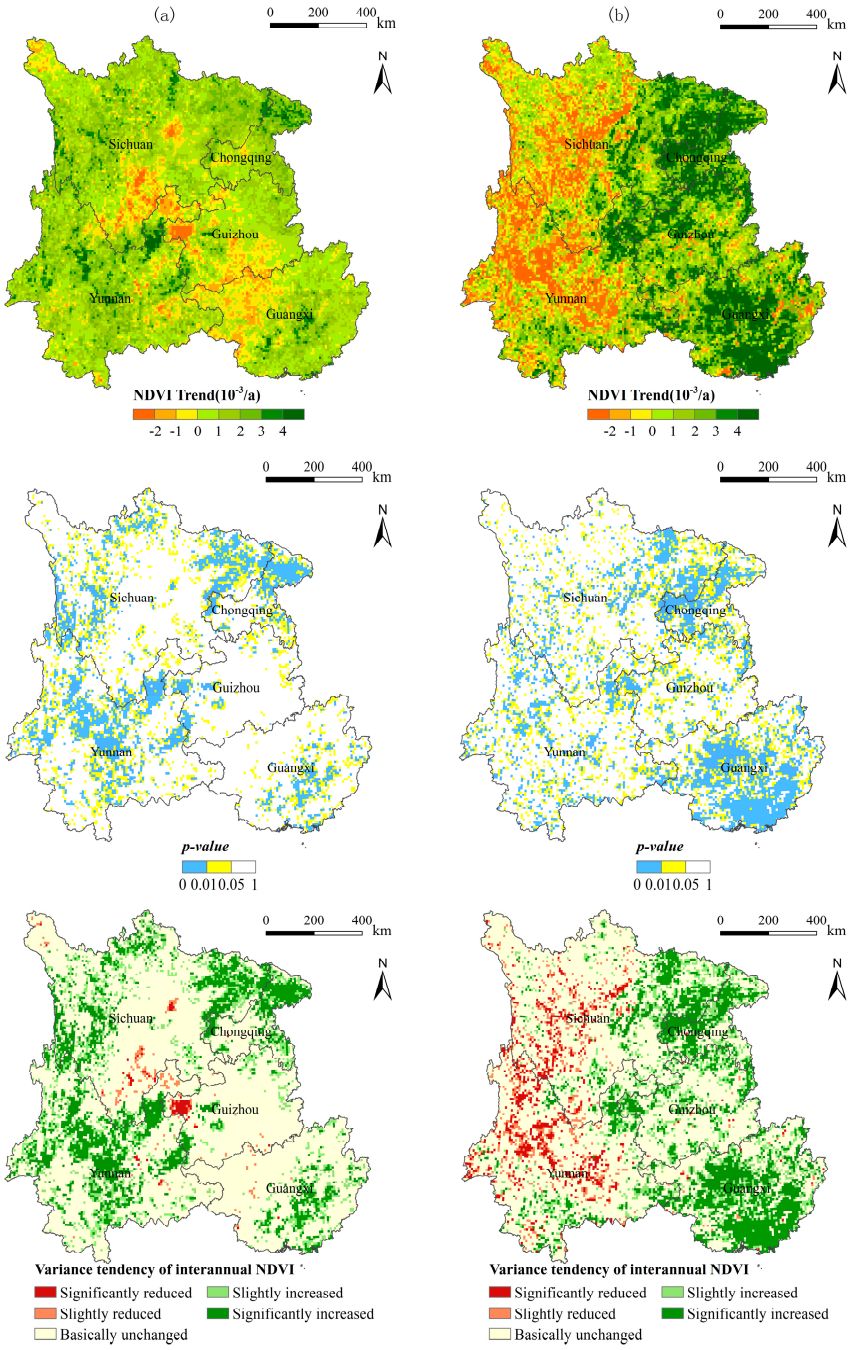

Figure 13. Comparison of spatial trend, the associated significance test and variance tendency over Southwest China between 1982–2000 (**a**) and 2001–2015 (**b**).

5. Conclusions

In the study, the spatiotemporal dynamics of vegetation and its driving factors over Southwest China during 1982–2015 were investigated. The results indicated that the multi-year mean NDVI over Southwest China from 1982 to 2015 showed a decreasing trend from the southeastern region to the northwestern region. Vegetation NDVI showed an overall significantly increasing trend, at a rate of 0.936×10^{-3}/a. Among the four vegetation types, NDVI trend of cultivated land, forest land, shrubland and grassland were 1.107×10^{-3}/a, 0.89×10^{-3}/a, 0.827×10^{-3}/a and 0.509×10^{-3}/a, respectively. The area proportions of significant and slight increase in NDVI accounted for 50.14% and 8.61%, respectively, whereas significant and slight reduction in NDVI only appeared in a small area by 3.29% and 2.49%, respectively. The eastern area was the main NDVI increased area. On the contrary, the western area was the main NDVI reduction area, especially in western Sichuan and northwestern and central Yunnan. Temperature was the dominant climate driving factor by about 48.19%, followed by downward shortwave radiation (3.71%) and precipitation (3.09%), respectively. Compared with the non-karst area (0.929×10^{-3}/a), the overall trend in the karst area was larger (1.035×10^{-3}/a). Moreover, the trend after 2000 was apparently stronger than that before 2000, indicated the importance of ecological restoration projects for the vegetation protection.

Author Contributions: C.D.: Formal analysis, investigation, data curation, writing; J.L.: Formal analysis, investigation; X.T., Z.D. and L.Y.: Methodology, resources; M.M. and Y.C.: Conceptualization, methodology; J.X.: Reviewing and editing; X.T.: Reviewing and funding. All authors have read and agreed to the published version of the manuscript.

Funding: This study was jointly supported by the Natural Science Foundation of China (41901145), the Special Project on National Science and Technology Basic Resources Investigation of China (Grant No. 2021FY100701) and the National Major Projects on High-Resolution Earth Observation System (Grant No. 21-Y20B01-9001-19/22).

Data Availability Statement: All data can be accessed through the provided website.

Acknowledgments: We are grateful to the developers of AVHRR GIMMS NDVI3g products provided by NASA Ames Ecological Forecasting Lab, CMFD produced by Big Earth Data for Three Poles, and GLASS China' s 1982–2018 0.05° land cover classification product developed by National Earth System Science Data Sharing Infrastructure, National Science and Technology Infrastructure of China.

Conflicts of Interest: The authors declare no conflict of interest.

References

1. Li, D.; Pan, M.; Cong, Z.; Zhang, L.; Wood, E. Vegetation control on water and energy balance within the Budyko framework. *Water Resour. Res.* **2013**, *49*, 969–976. [CrossRef]
2. Nemani, R.R.; Keeling, C.D.; Hashimoto, H.; Jolly, W.M.; Piper, S.C.; Tucker, C.J.; Myneni, R.B.; Running, S.W. Climate-Driven Increases in Global Terrestrial Net Primary Production from 1982 to 1999. *Science* **2003**, *300*, 1560–1563. [CrossRef] [PubMed]
3. Piao, S.; Wang, X.; Ciais, P.; Ciais, P.; Zhu, B.; Wang, T.; Liu, J. Changes in satellite-derived vegetation growth trend in temperate and boreal Eurasia from 1982 to 2006. *Glob. Chang. Biol.* **2011**, *17*, 3228–3239. [CrossRef]
4. Chen, B.; Xu, G.; Coops, N.C.; Ciais, P.; Myneni, R.B. Satellite-observed changes in terrestrial vegetation growth trends across the Asia Pacific region associated with land cover and climate from 1982 to 2011. *Int. J. Digit. Earth* **2016**, *9*, 1055–1076. [CrossRef]
5. Wu, D.; Zhao, X.; Liang, S.; Zhou, T.; Huang, K.; Tang, B.; Zhao, W. Time-lag effects of global vegetation responses to climate change. *Glob. Chang. Biol.* **2015**, *21*, 3520–3531. [CrossRef]
6. Zhang, Y.; Ye, A. Spatial and temporal variations in vegetation coverage observed using AVHRR GIMMS and Terra MODIS data in the mainland of China. *Int. J. Remote Sens.* **2020**, *41*, 4238–4268. [CrossRef]
7. Anyamba, A.; Tucker, C.J. Analysis of Sahelian vegetation dynamics using NOAA-AVHRR NDVI data from 1981–2003. *J. Arid Environ.* **2005**, *63*, 596–614. [CrossRef]
8. Jiang, W.; Yuan, L.; Wang, W.; Wang, W.; Cao, R.; Zhang, Y.; Shen, W. Spatio-temporal analysis of vegetation variation in the Yellow River Basin. *Ecol. Indic.* **2015**, *51*, 117–126. [CrossRef]
9. Beck, H.E.; McVicar, T.R.; Dijk, A.I.J.M.; Schellekens, J.; de Jeu, R.A.M.; Bruijinzeel, L.A. Global evaluation of four AVHRR–NDVI data sets; Intercomparison and assessment against Landsat imagery. *Remote Sens. Environ.* **2011**, *115*, 2547–2563. [CrossRef]
10. Tucker, C.J.; Townshend, J.R.G.; Goff, T.E. African land-cover classification using satellite data. *Science* **1985**, *227*, 369–375. [CrossRef]

11. Hunt, E.R. Relationship between woody biomass and PAR conversion efficiency for estimating net primary production from NDVI. *Int. J. Remote Sens.* **1994**, *15*, 1725–1729.
12. Fensholt, R.; Langanke, T.; Rasmussen, K.; Reenberg, A.; Prince, S.D.; Tucker, C.J.; Scholes, R.J.; Quang, B.; Bondeau, A.; Eastman, R.; et al. Greenness in semi-arid areas across the globe 1981–2007—An Earth Observing Satellite based analysis of trends and drivers. *Remote Sens. Environ.* **2012**, *121*, 144–158. [CrossRef]
13. Scheftic, W.; Zeng, X.; Broxton, P.; Brunke, M. Intercomparison of seven NDVI products over the United States and Mexico. *Remote Sens.* **2014**, *6*, 1057–1084. [CrossRef]
14. Chang, Q.; Zhang, J.; Jiao, W.; Yao, F. A comparative analysis of the NDVIg and NDVI3g in monitoring vegetation phenology changes in the Northern Hemisphere. *Geocarto Int.* **2018**, *33*, 1–20. [CrossRef]
15. Jiang, N.; Zhu, W.; Zheng, Z.; Chen, G.; Fan, D. A Comparative Analysis between GIMSS NDVIg and NDVI3g for Monitoring Vegetation Activity Change in the Northern Hemisphere during 1982–2008. *Remote Sens.* **2013**, *05*, 4031–4044. [CrossRef]
16. Du, J.; Shu, J.; Zhao, C.; Ahati, J.; Wang, L.; Xiang, B.; Fang, G.; Liu, W.; He, P. Comparison of GIMMS NDVI3g and GIMMS NDVIg for monitoring vegetation activity and its responses to climate changes in Xinjiang during 1982-2006. *Acta Ecol. Sin.* **2016**, *36*, 6738–6749.
17. Vicente-Serrano, S.M.; Gouveia, C.; Camarero, J.J.; Beguería, S.; Trigo, R.; López-Moreno, J.I.; Azorín-Molina, C.; Pasho, E.; Lorenzo-Lacruz, J. Response of vegetation to drought time-scales across global land biomes. *Proc. Natl. Acad. Sci. USA* **2013**, *110*, 52–57. [CrossRef]
18. Zhang, Y.; Zhang, C.; Wang, Z.; Chen, Y.; Gang, C.; An, R.; Li, J. Vegetation dynamics and its driving forces from climate change and human activities in the Three-River Source Region, China from 1982 to 2012. *Sci. Total Environ.* **2016**, *563*, 210–220. [CrossRef]
19. Jiang, L.; Jiapaer, G.; Bao, A.; Guo, H.; Ndayisaba, F. Vegetation dynamics and responses to climate change and human activities in Central Asia. *Sci. Total Environ.* **2017**, *599*, 967–980. [CrossRef]
20. Wang, S.; Li, R.; Wu, Y.; Zhao, S. Vegetation dynamics and their response to hydrothermal conditions in Inner Mongolia, China. *Glob. Ecol. Conserv.* **2022**, *34*, e02034. [CrossRef]
21. Su, W. Controlling Model for Rocky Desertification of Karst Mountainous Region and Its Preventing Strategy in Southwest China. *J. Soil Water Conserv.* **2002**, *16*, 29–32, 79.
22. Ding, Z.; Zheng, H.; Liu, Y.; Zeng, S.; Yu, P.; Shi, W.; Tang, X. Spatiotemporal Patterns of Ecosystem Restoration Activities and Their Effects on Changes in Terrestrial Gross Primary Production in Southwest China. *Remote Sens.* **2021**, *13*, 1209. [CrossRef]
23. Tang, X.; Xiao, J.; Ma, M.; Yang, H.; Li, X.; Ding, Z.; Yu, P.; Zhang, Y.; Wu, C.; Jing, H.; et al. Satellite evidence for China's leading role in restoring vegetation productivity over global karst ecosystems. *For. Ecol. Manag.* **2022**, *507*, 120000. [CrossRef]
24. Wang, M.; Ding, Z.; Wu, C.; Song, L.; Ma, M.; Yu, P.; Lu, B.; Tang, X. Divergent responses of ecosystem water-use efficiency to extreme seasonal droughts in Southwest China. *Sci. Total Environ.* **2021**, *760*, 143427. [CrossRef]
25. Nie, Y.; Chen, H.; Wang, K.; Yang, J. Water source utilization by woody plants growing on dolomite outcrops and nearby soils during dry seasons in karst region of Southwest China. *J. Hydrol.* **2012**, *420*, 263–274. [CrossRef]
26. Pinzon, J.E.; Tucker, C.J. A Non-Stationary 1981-2012 AVHRR NDVI3g Time Series. *Remote Sens.* **2014**, *06*, 6929–6960. [CrossRef]
27. Tucker, C.J.; Pinzon, J.E.; Brown, M.; Slayback, D.A.; Pak, E.W.; Mahoney, R.; Vermote, E.F.; Saleous, N.E. An extended AVHRR 8-km NDVI dataset compatible with MODIS and SPOT vegetation NDVI data. *Int. J. Remote Sens.* **2005**, *26*, 4485–4498. [CrossRef]
28. Fensholt, R.; Proud, S.R. Evaluation of Earth Observation based global long term vegetation trends—Comparing GIMMS and MODIS global NDVI time series. *Remote Sens. Environ.* **2012**, *119*, 131–147. [CrossRef]
29. Huete, A.; Didan, K.; Miura, T.; Rodriguez, E.P.; Gap, X.; Ferreira, L.G. Overview of the radiometric and biophysical performance of the MODIS vegetation indices. *Remote Sens. Environ.* **2002**, *83*, 195–213. [CrossRef]
30. Zeng, F.; Collatz, G.J.; Pinzon, J.E.; Ivanoff, A. Evaluating and Quantifying the Climate-Driven Interannual Variability in Global Inventory Modeling and Mapping Studies (GIMMS) Normalized Difference Vegetation Index (NDVI3g) at Global Scales. *Remote Sens.* **2013**, *5*, 3918–3950. [CrossRef]
31. Yang, K.; He, J.; Tang, W.; Qin, J.; Cheng, C. On downward shortwave and longwave radiations over high altitude regions; Observation and modeling in the Tibetan Plateau. *Agric. For. Meteorol.* **2010**, *150*, 38–46. [CrossRef]
32. He, J.; Yang, K.; Tang, W.; Lu, H.; Qin, J.; Chen, Y.; Li, X. The first high-resolution meteorological forcing dataset for land process studies over China. *Sci. Data* **2020**, *7*, 25. [CrossRef] [PubMed]
33. Wang, H.; Zhao, X.; Zhang, X.; Wu, D.; Du, X. Long Time Series Land Cover Classification in China from 1982 to 2015 Based on Bi-LSTM Deep Learning. *Remote Sens.* **2019**, *11*, 1639. [CrossRef]
34. Carreiras, J.M.B.; Pereira, J.M.C.; Shimabukuro, Y.E.; Stroppiana, D. Evaluation of compositing algorithms over the Brazilian Amazon using SPOT-4 VEGETATION data. *Int. J. Remote Sens.* **2003**, *24*, 3427–3440. [CrossRef]
35. Holben, B.N. Characteristics of maximum-value composite images from temporal AVHRR data. *Int. J. Remote Sens.* **1986**, *7*, 1417–1434. [CrossRef]
36. Sobrino, J.; Julien, Y. Global trends in NDVI-derived parameters obtained from GIMMS data. *Int. J. Remote Sens.* **2011**, *32*, 4267–4279. [CrossRef]
37. Xu, G.; Zhang, H.; Chen, B.; Zhang, H.; Innes, J.L.; Wang, G.; Yan, J.; Zheng, Y.; Zhu, Z.; Myneni, R.B. Changes in Vegetation Growth Dynamics and Relations with Climate over China's Landmass from 1982 to 2011. *Remote Sens.* **2014**, *6*, 3263–3283. [CrossRef]

38. Li, S.; Yang, S.; Liu, X.; Liu, Y.; Shi, M. NDVI-Based Analysis on the Influence of Climate Change and Human Activities on Vegetation Restoration in the Shaanxi-Gansu-Ningxia Region, Central China. *Remote Sens.* **2015**, *7*, 11163–11182. [CrossRef]
39. Lü, Y.; Zhang, L.; Yan, H.; Ren, X.; Wang, J.; Niu, Z.; Gu, F.; He, H. Spatial and temporal patterns of changing vegetation and the influence of environmental factors in the karst region of Southwest China. *Acta Ecol. Sin.* **2018**, *38*, 8774–8786.
40. Yang, Y.; Hou, Z.; Zhang, Z. NDVI Changes and Driving Factors in Southwest China from 2001 to 2018. *Bull. Soil Water Conserv.* **2021**, *41*, 337–344.
41. Chen, W.; Bai, S.; Zhao, H.; Han, X.; Li, L. Spatiotemporal analysis and potential impact factors of vegetation variation in the karst region of Southwest China. *Environ. Sci. Pollut. Res.* **2021**, *28*, 61258–61273. [CrossRef] [PubMed]
42. Qiao, Y.; Jiang, Y.; Zhang, C. Contribution of karst ecological restoration engineering to vegetation greening in southwest China during recent decade. *Ecol. Indic.* **2021**, *121*, 107081. [CrossRef]
43. Wang, J.; Meng, J.; Cai, Y. Assessing vegetation dynamics impacted by climate change in the southwestern karst region of China with AVHRR NDVI and AVHRR NPP time-series. *Environ. Geol.* **2008**, *54*, 1185–1195. [CrossRef]
44. Zhou, J.; Ma, M.; Xiao, Q.; Wem, J. Vegetation Dynamics and Its Relationship with Climatic Factors in Southwest China. *Remote Sens. Technol. Appl.* **2017**, *32*, 966–972.
45. Xiao, J.; Wang, S.; Bai, X.; Zhou, D.; Tian, Y.; Li, Q.; Wu, L.; Qian, Q.; Chen, F.; Zeng, C. Determinants and spatial-temporal evolution of vegetation coverage in the karst critical zone of South China. *Acta Ecol. Sin.* **2018**, *38*, 8799–8812.
46. Mao, Y.; Jiang, Y.; Zhang, C.; Qiao, Y.; Lü, T.; Qiu, J. Spatio-temporal Changes and Influencing Factors of Vegetation Net Primary Productivity in Southwest China in the Past 20 years and Its Response to Ecological Engineering. *Acta Ecol. Sin.* **2022**, *42*, 2878–2890.
47. Tao, J.; Xu, T.; Dong, J.; Yu, X.; Jiang, Y.; Zhang, Y.; Huang, K.; Zhu, J.; Dong, J.; Xu, Y. Elevation-dependent effects of climate change on vegetation greenness in the high mountains of southwest China during 1982–2013. *Int. J. Climatol.* **2018**, *38*, 2029–2038. [CrossRef]
48. Cao. Impact of China's Large-Scale Ecological Restoration Program on the Environment and Society in Arid and Semiarid Areas of China; Achievements, Problems, Synthesis, and Applications. *Crit. Rev. Environ. Sci. Technol.* **2011**, *41*, 317–335. [CrossRef]
49. Zhang, X.; Yue, Y.; Tong, X.; Wang, K.; Qi, X.; Deng, C.; Brandt, M. Eco-engineering controls vegetation trends in southwest China karst. *Sci. Total Environ.* **2021**, *770*, 145160. [CrossRef]
50. Wu, L.; Wang, S.; Bai, X.; Tian, Y.; Luo, G.; Wang, J.; Li, Q.; Chen, F.; Deng, Y.; Yang, Y. Climate change weakens the positive effect of human activities on karst vegetation productivity restoration in southern China. *Ecol. Indic.* **2020**, *115*, 106392. [CrossRef]
51. Zheng, Z.; Zeng, Y.; Zhao, Y.; Gao, W.; Zhao, D.; Wu, B. Analysis of land cover changes in southwestern China since the 1990s. *Acta Ecol. Sin.* **2016**, *36*, 7858–7869.
52. Zhao, H.; Wu, R.; Yang, F.; Hu, J.; Wang, J.; Guo, Y.; Feng, Z.; Zhang, C.; Wang, Y.; Zhou, J. Spatiotemporal patterns of vegetation conversion under the Grain for Green Program in southwest China. *Conserv. Sci. Pract.* **2021**, *4*, e604. [CrossRef]
53. Wang, M.; Wang, W.; Li, J.; Wu, H.; Cu, C.; Liu, T. The Impact of Sustained Drought on Vegetation Ecosystem in Southwest China Based on Remote Sensing. In Proceedings of the International Conference on Ecological Informatics and Ecosystem Conservation (ISEIS 2010), Beijing, China, 27–29 August 2010; Volume 2, pp. 1679–1691.
54. Liu, B.; Li, Y.; Chen, J.; Chen, X. Long-term change in precipitation structure over the karst area of southwest China. *Int. J. Climatol.* **2016**, *36*, 2417–2434. [CrossRef]
55. Li, X.; He, B.; Quan, X.; Liao, Z.; Bai, X. Use of the Standardized Precipitation Evapotranspiration Index (SPEI) to Characterize the Drying Trend in Southwest China from 1982–2012. *Remote Sens.* **2015**, *7*, 10917–10937. [CrossRef]
56. Chen, X.; Chen, T.; Yan, Q.; Cai, J.; Guo, R.; Gao, M.; Wei, X.; Zhou, S.; Li, C.; Xie, Y. The Ongoing Greening in Southwest China despite Severe Droughts and Drying Trends. *Remote Sens.* **2021**, *13*, 3374. [CrossRef]
57. Brandt, M.; Yue, Y.; Wigneron, J.; Tong, X.; Tian, F.; Jesper, M.R.; Xiao, X.; Verger, A.; Mialon, A.; Al-Yaani, A. Satellite-observed major greening and biomass increase in South China karst during recent decade. *Earth's Future* **2018**, *6*, 1017–1028. [CrossRef]
58. Jin, K.; Wang, F.; Han, J.; Shi, S.; Ding, W. Contribution of climatic change and human activities to vegetation NDVI change over China during 1982-2015. *Acta Geogr. Sin.* **2020**, *75*, 961–974.
59. Zhang, Y.; Peng, C.; Li, W.; Tian, L.; Zhu, Q.; Chen, H.; Fang, X.; Zhang, G.; Liu, G.; Mu, X. Multiple afforestation programs accelerate the greenness in the 'Three North' region of China from 1982 to 2013. *Ecol. Indic.* **2016**, *61*, 404–412. [CrossRef]
60. Peng, J.; Jiang, H.; Liu, Q.; Green, S.M.; Quine, T.A.; Liu, H.; Qiu, S.; Liu, Y.; Meersmans, J. Human activity vs. climate change; Distinguishing dominant drivers on LAI dynamics in karst region of southwest China. *Sci. Total Environ.* **2021**, *769*, 144297. [CrossRef]